

## HALOGEN-FREE FLAME-RETARDANT POWDER MATERIALS FOR LASER SINTERING: EVALUATION AND PROCESS STABILITY ANALYSIS

F. Neitzel\*, I. Kletetzka\*, H.-J. Schmid\*

\*Direct Manufacturing Research Center (DMRC) and Particle Technology Group,  
Paderborn University, Germany

### Abstract

The high flammability of components manufactured by laser-based powder bed fusion of plastics (PBF-LB/P) using standard polyamide 12 (PA12) powder still severely restricts their use in industries such as electronics, aviation, and transportation. A key factor for the further establishment of PBF-LB/P is the expansion of the material portfolio with, for example, refreshable and halogen-free flame-retardant (FR) powder materials. Accordingly, various halogen-free FRs are investigated in this work and evaluated with respect to their use in PBF-LB/P. First, their decomposition behavior and mode of action are examined. Subsequently, the additives are dry blended with PA12 to investigate properties relevant for PBF-LB/P, such as particle morphology, thermal behavior, and melt viscosity. Afterwards, test specimens for UL94 vertical flame-retardancy tests are produced by processing the dry blends on an EOS P3 PBF-LB/P system. Finally, the process stability of the process-aged powder blends is investigated by again examining thermal behavior and melt viscosity.

### Introduction

In the context of additive manufacturing (AM), laser-based powder bed fusion of plastics (PBF-LB/P), here referred to as laser sintering (LS), is one of the most important technologies for processing engineering plastics. In this process, a thin layer of thermoplastic powder is coated on a build platform, preheated and locally melted by a laser. Afterwards the platform is lowered by the height of a single layer and the next iteration of the process starts. This cycle is repeated until every layer of the component is finished. Since the development of this process more than 30 years ago, LS has developed into a technology that not only enables functional prototyping but has also recently been increasingly used for industrial series production. Nevertheless, the number of suitable materials is still severely limited, which means that not all customer requirements can be met. An example for this often-conflicting requirements is the flame-retardancy of polymer LS materials, which is required for aviation, medical, electronics and many more industries. Currently, commercially available flame-retardant (FR) LS powders either contain hazardous halogenated additives or the reuse of process-aged powder is not possible. [1]

In the past, many general investigations on the flame-retardancy of polyamide in combination with various FRs have been conducted [2–4]. However, studies focusing on the development of FR materials for LS are limited. A review on the use of various FRs showed that currently only halogen- and phosphorous-based additives are used in AM, while other groups of FR additives have mostly been neglected [5]. In most of these investigations the goal was to increase the flame-retardancy to fulfill the requirements of a better FR classification. For example,

halogen-free phosphinate-based FRs with different filling ratios were examined and showed that high filling ratios of 25 wt% were needed to achieve a UL-94 rating of V-1. However, this high filler content leads to limitations in processing and to a reduction in the mechanical part properties [6]. Besides this difficult compromise of flame-retardancy and good mechanical properties, the high amount of FR PA12 waste powder is especially problematic. Typically, only a small portion of powder is used to fabricate parts. According to the material supplier *EOS GmbH - Electro Optical Systems (EOS)* and *3D Systems*, only the use of virgin powder is recommended, as components made from used powder do not have the same FR properties. Therefore, all excess FR powder cannot be used for further sintering processes and is usually disposed of after one process iteration [7, 8]. Regarding recyclability it was recently found that aged PA12 powder with 15 wt% of organic phosphinates in combination with 1 wt% of nanoclay achieved a UL94 standard rating of V-0 (3 mm), while enhancing tensile and impact properties [9]. Whereby, the process stability of the FRs for a further reuse of process aged powder was not part of the investigation. To develop a recyclable FR LS material in the future, suitable FR additives need to be determined. The aim of this work is therefore the investigation and evaluation of various halogen-free FRs in combination with a PA12 matrix for the usage in LS, while taking the process stability into account.

To assess whether a particular FR additive is suitable for LS, general requirements, or key properties for LS powder materials must first be set. Based on these key properties, selection criteria for FRs are then defined before a selection of technically suitable agents is made. Basically, the most important properties of LS polymers can be divided into extrinsic and intrinsic properties. The former includes particle size, particle morphology and powder behavior. The latter includes optical, rheological, and thermal properties. Apart from this, the synthesis and basic structure of the polymer is also one of the key properties but is not part of the investigations within this work since the focus is on adding FRs to a commercially available polymer material. The following Table 1 provides an overview of the key properties of polymers for LS. [10]

*Table 1: Overview of the key properties for LS polymers [10]*

Extrinsic		Intrinsic	
Properties	Specifics	Properties	Specifics
Particle morphology	Particle shape	Rheological properties	Melt viscosity
	Surface properties		Surface tension
Powder behavior	Production method	Thermal properties	Melting point
	Particle size distribution		Crystallization
			Powder rheology
		Heat capacity	
		Optical properties	Absorption
			Reflection

Since not all material requirements are equally important in an additive application, this work focuses on the powder behavior, rheological, and thermal properties of different FR powder blends. As there is a wide variety of FR additives available for polymers, it is necessary to establish selection criteria for decision making, based on the key properties for LS. These defined criteria are as follows:

The **FR composition** must only contain halogen-free additives due to restrictions on the use of halogens in e.g., electronic components due to their persistence, bioaccumulation, and toxicity in the environment. Since the base material used in this work is a PA12, the additive should be as compatible as possible. The selected additives should have synergistic effects with other FRs to increase the effectiveness and reduce the amount of additive required. [11, 12]

The **decomposition temperature** of the FRs must be higher than the temperature of the build chamber (approx. 178 °C) and the peak melt pool (approx. 270 °C [13]) to maintain the FR mechanism. In addition, the FR mechanism should start before the polymer decomposes (approx. 360 °C for PA12) and, if possible, extend over the entire decomposition area.

The **particle size** of each FR should be larger than 5 µm to avoid cohesive flow behavior and to ensure good coating results during LS as well as good dry mixability. If the FR additive is incorporated into the polymer particle for example by melt mixing, smaller particles could be used as well. Due to the maximum layer thickness of the EOS P3 machines to be used, the particle size must be less than 180 µm, to avoid scoring during coating. For the most efficient process regarding process duration and part quality a layer height of 120 µm is preferred.

## Materials

Since the LS market is still dominated by PA12 materials the intended approach is to produce FR materials by dry blending various combinations of FRs with PA12 powder. As a matrix material a **PA12** powder (INFINAM PA 6002 P by *Evonik*) with improved reusability was selected. The powder exhibits a distinct processing window between the onset of melting (melting point after initial heating at 186.5 °C) and crystallization (maximum peak at 142.5 °C). The volumetric median particle size of the material is 58 µm. For the conducted investigations 100 % virgin powder was used.

Based on the criteria established in the previous section and with the aim of covering each relevant group of halogen-free FRs as much as possible, the following additives were selected within the scope of this work [5, 14]:

### **Aluminum hydroxide** (Apyral 40CD – *Nabaltec*)

Apyral 40CD is aluminum hydroxide, also called aluminum trihydrate (ATH), and is manufactured by *Nabaltec AG*. When the temperature threshold of approx. 240 °C is reached, ATH decomposes into aluminium oxide and water. During this endothermic reaction, energy is consumed from the ignition source and at the same time the aluminum oxide forms a protective layer. According to the manufacturer, the specific density is 2.4 g/cm<sup>3</sup> and 90 % of the particles are smaller than 3.3 µm. To meet the requirements for a UL94-V0 rating, high fill rates of about 50 wt% are usually required. [15, 16]

### **Boehmite** (Actilox B30 – *Nabaltec*)

*Nabaltec AG* is also the manufacturer of Actilox B30, an aluminum oxide hydroxide also known as aluminum monohydrate (AOH) or boehmite. The FR mechanism is comparable to that of ATH, but AOH contains less crystal-bound water, which in turn leads to a significant increase in temperature stability. Thus, the decomposition of AOH starts at 340 °C. Due to its lower energy consumption during decomposition, boehmite is often used as a synergist with, for example,

phosphorus or nitrogen systems. *Nabaltec* states that the specific density is 3 g/cm<sup>3</sup> and 50 % of the particles are smaller than 2.3 μm. [15]

**Magnesium hydroxide** (Versamag – *Martin Marietta*)

Under the trade name Versamag, the *Martin Marietta* company sells magnesium hydroxide, which, like boehmite, also releases water through endothermic decomposition at about 330 °C. This produces a cooling effect, reduces oxygen availability, and suppresses smoke formation. The endothermic reaction also produces magnesium oxide ash, which forms a protective layer. The specific density is approx. 2.36 g/cm<sup>3</sup> and the particle size is in a range of 2 μm – 4 μm. [17]

**Organic phosphinate** (Exolit OP1400 – *Clariant*)

Exolit OP1400 is a synergistic FR blend produced by *Clariant* with aluminum diethyl phosphinate (Depal) as the main component and another unknown phosphorus component. Due to the P-P synergy, a significant charring effect is observed with polyamides in flame tests. However, it is likely that a gas-phase mechanism of action is also present. OP1400 was developed for use in polyamides and is therefore temperature stable up to 340 °C. 90 % of the particles of the additive are smaller than 53 μm and the specific density is approx. 1.45 g/cm<sup>3</sup>. [18, 19]

**Melamine cyanurate** (Aflammit PMN525 – *THOR* / Nord-Min MC-25J – *Nordmann*)

Since melamine cyanurate is used as a standard for unfilled polyamide plastics, the two FRs to be investigated in this project are Aflammit PMN525 from *THOR* and Nord-Min MC-25J from *Nordmann*. Analogous to the phosphorus-containing systems, these two additives also form a protective layer by charring. In addition, both have extremely low water solubility, are thermostable up to approx. 300 °C and have a specific density of 1.7 g/cm<sup>3</sup>. The particle size of PMN525 (98 % smaller than 8 μm) is significantly smaller (98 % smaller than 25 μm) compared to MC-25J. [20, 21]

**Zinc borate** (Aflammit PCI511 – *THOR*)

*THOR* also sells a zinc borate called Aflammit PCI511. This is mainly used as a synergist for intumescent systems, where PCI511 improves the structure of the protective layer and can act as an anti-drip agent. The additive is temperature stable up to approx. 300 °C and has a specific density of 0.28 g/cm<sup>3</sup>. The size of 50 % of the particles is below 10 μm. [22]

**Borosilicate glass foam** (TROVO powder B – *Trovotech*)

*Trovotech* has developed TROVO powder B, a material consisting of an amorphous borosilicate glass powder. This is to be used primarily as a synergist in nitrogen as well as phosphorus FRs and, when exposed to flame, to support the formation of the intumescent layer by vitrification of the polymer. Processing is said to be possible up to 280 °C and the size of 90 % of the particles is less than 9 μm. The manufacturer does not provide more detailed information on the specific density. [23, 24]

**Expandable graphite** (GHL PX90-1HT – *Luh*)

GHL PX90-2 is an expandable graphite produced by the *Luh* company. When a temperature threshold is reached, blowing agents cause the individual graphite layers of the FR to expand and form a voluminous and thermally stable char layer. Typically, expandable graphite is used as a synergist to stabilize the substrate and reduce flammability. The fire protection properties of the additive depend to a large extent on the particle size, as the protective layer formed also decreases

with decreasing particle size. In this case, 75 % of the particles are smaller than 150  $\mu\text{m}$ , which is also the finest variant in the product range. The manufacturer states that at approx. 230  $^{\circ}\text{C}$  – 250  $^{\circ}\text{C}$  the expansion process of the graphite begins. The specific density is not known. [25, 26]

Typically, as the particle size decreases, the importance of van der Waals forces increases, leading to increased formation of agglomerates and thus reduced powder flowability. These agglomerates cannot be completely broken up during mixing with a drum ring mixer, which can lead to an inhomogeneous distribution of the additives and therefore reduced flame-retardancy. For this reason, a high intensity laboratory mixer (EL5 by *EIRICH*) was used. Each dry blend consisting of the PA12 matrix material and one or more of the previously introduced FRs was mixed at 500 rpm for 10 min. [10]

### **Experimental Methods**

The decomposition behavior of the various FRs was investigated by **thermogravimetric analysis (TGA)**. The analyses were carried out with an TGA/DSC 1 (Star System) of the company *Mettler-Toledo AG* according to the DIN EN ISO 11358-1 standard. The specimens with a sample mass of approx. 30 mg were heated with a set rate of 10 K/min under nitrogen atmosphere up to 600  $^{\circ}\text{C}$ . The specimen chamber is then flooded with oxygen and heated up to 1000  $^{\circ}\text{C}$  to burn out residual materials and impurities. During the analysis the change in mass is measured as a function of temperature. [27]

**Particle size distribution (PSD)** was measured by dynamic image analysis using a QICPIC by *Sympatec* according to ISO 13322-2. Within the dynamic image analysis, a digital camera captures the particle collective flowing continuously through the measurement volume and can thus record the actual shape and size distribution. The measuring range was set to M5, therefore particle sizes in between 1.8 and 3755  $\mu\text{m}$  were measurable. A dry dispersion unit was used to break up the particle collective. [28, 29]

To investigate the melt viscosity at a given shear rate, the **melt volume flow rate (MVR)** was determined using a capillary rheometer from *Zwick Roell*. The test series was carried out in accordance with DIN EN ISO 1133-1. For this purpose, a sample mass of approx. 4 g of the material to be tested was filled into a heated cylinder. The specimen was melted for 5 min. The melt was then extruded through a fixed diameter die by a piston with a defined test weight. To measure MVR, the length of the distance traveled by the piston in a given time, or the time required for the piston to travel a given distance, was recorded, and used to calculate the extrusion rate in  $\text{cm}^3/10 \text{ min}$ . The test temperature was set at 220  $^{\circ}\text{C}$  with a test weight of 10 kg for all tests. To avoid falsification of the measurement results due to moisture in the polymer, the samples were first dried in a laboratory oven at 105  $^{\circ}\text{C}$  for 30 min. The MVR was calculated from the average of at least three samples per material tested. [30]

The analysis of the thermal behavior especially the processing window of each dry blend was carried out using **differential scanning calorimetry (DSC)**. Within the scope of this work, the measurement according to DIN EN ISO 11357-1 was carried out with the DSC 214 Polyma measuring instrument from *Netzsch*. During the measurement, the sample and a reference are subjected to the same temperature program. The difference in the heat flows is measured, which provides information about the melting and crystallization behavior of the plastic, for example. In

these investigations, the samples were heated to 230 °C at a heating and cooling rate of 10 K/min. The sample mass was 10±0.3 mg. [31]

Basically, a fire protection classification of plastics can be carried out according to the **UL94** regulations of the American *Underwriters Laboratories*. The test was carried out on a test bars (80 x 12.5 x 3 mm) with a methane gas flame of 50 W and a flame length of 20 mm. In the vertical fire test, the test specimen was flamed twice for 10 s each. After each flame treatment, the burning duration, and the dripping of burning material were evaluated with the aid of a cotton swab. The specimens were pretreated at 70 °C for 7 days in a hot air oven. Depending on the burning time and dripping of the burning material, the classification was made according to the thickness into flammability classes V-0, V-1, V-2, where V-0 is the best classification. Table 2 shows the criteria and classification of the materials rating in the UL94 V test. For each dry blend at least five specimens were tested. [32]

Table 2: Criteria for flame-retardancy classification in UL94 vertical tests [32]

Criteria for sample classification	V-0	V-1	V-2
Burning duration for each individual specimen after first or second ignition	≤ 10 s	≤ 30 s	≤ 30 s
Total burning duration for any set of five specimens after both ignitions	≤ 50 s	≤ 250 s	≤ 250 s
Glow duration after for each individual specimen after second ignition	≤ 30 s	≤ 60 s	≤ 60 s
Complete burnup of the specimen until clamping	No	No	No
Ignition of cotton wool indicator by burning dripping of the specimen	No	No	Yes

## Results

In this work the basic procedure for evaluating FRs regarding a suitable LS application as well as process stability is divided into five steps as shown in Figure 1. After each step the FRs respectively the dry blends are evaluated to determine if the step specific requirements are met. Specimens which don't fulfill the requirements won't be included in the following examinations.

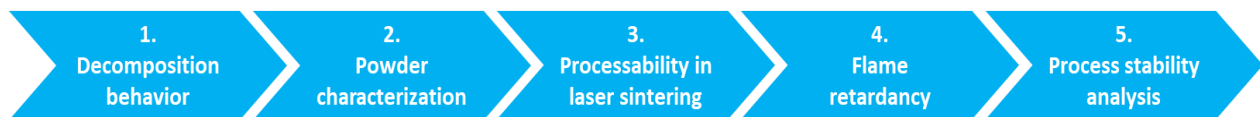


Figure 1: Methodology for evaluation process

First the decomposition behavior of the selected FRs was studied to determine if the additive can withstand the laser induced temperatures during the LS process. For test specimen production in the following third step the area energy density was set to 0.0288 J/mm<sup>2</sup> at which the expected melt pool temperature is approx. 270 °C [13]. Accordingly, the decomposition and therefore mode of action of the FRs to be part of further examinations must start at higher temperatures. For a FR to be processable in LS a weight loss of 1 % was set as the limit in this work which should not be exceeded at a temperature lower than the expected melt pool temperature. The decomposition behavior was investigated by TGA-analysis and the temperatures of each FR at a weight loss of 1 % and 5 % are given in Table 3.

These results clearly show that aluminum hydroxide (Apyral 40CD) reached the weight loss limit of 1 % at approx. 234 °C. At 268 °C at least 5 % of the test specimen weight was lost

thus indicating that this additive will most likely decompose to a certain amount during the LS process at the set energy density and consequently won't be suitable for a future LS-FR-powder application. The borosilicate glass foam (Trovopowder B-K3) was the first additive to reach a weight loss greater than 1 % at 208 °C. Due to the fact, that afterwards this FR can withstand much higher temperatures until a weight loss greater than 5 % occurred (293 °C), it still will be considered for the next evaluation step.

*Table 3: Temperature of each FR when reaching a weight loss greater than 1 % and 5 % determined by TGA under nitrogen atmosphere (up to 600 °C)*

Flame-retardant	Content	Weight loss > 1 % / °C	Weight loss > 5 % / °C
Trovopowder B-K3	Borosilicate glass foam	208.00	292.67
Apyral 40CD	Aluminum hydroxide	234.17	267.67
GHL PX 90/-2	Expandable graphite	276.50	307.00
Aflammit PCI 511	Zinc borate	300.50	379.33
Nord-Min MC-25J	Melamine cyanurate	320.17	350.50
Versamag	Magnesium hydroxide	323.83	356.67
Aflammit PMN 525	Melamine cyanurate	326.83	345.33
Exolit OP 1400	Organic phosphinate	382.17	404.50
Actilox B30	Boehmite	393.00	511.67

In the following Figure 2 the results of the TGA-analysis of selected FRs in comparison to virgin PA12 powder (PA 6002 P VP) and the approximate melt pool temperature (270 °C) are given. Here, the percentage weight loss is documented as a function of temperature. Analogous to the previous description the decomposition of aluminum hydroxide has already begun before reaching the assumed melt pool temperature. After losing about 30 % of the sample weight due to the release of water 70 % of the sample weight remain as a residue mostly consisting of aluminum oxide. When looking at the behavior of the borosilicate glass foam it is noticeable that this additive has decomposed to a small extent at 270 °C but most of it remains stable until reaching approx. 280 °C. When the decomposition of this additive is done, about 45 % of the sample weight remain as a glass foam residue. Basically, to increase the flame-retardancy of a polymer by using FRs, the decomposition of these additives should preferably start at the same time or just before the decomposition of the polymer to achieve the highest efficiency [33]. This applies to melamine cyanurate (Aflammit PMN525) and the organic phosphinate (Exolit OP1400) and therefore the assumption is made that these FRs will achieve the best flame-retardancy in a PA12 application. After the decomposition of phosphinate a carbonaceous foam remains as residue. The melamine-based FR as well as the virgin PA12 powder (PA 6002 P VP) decomposed almost residue-free. Compared to aluminum hydroxide boehmite (Actilox B30) contains less releasable crystal-bound water which is why the thermal stability is higher and less weight is lost during decomposition. Also, about 85 % of the sample mass remain as aluminum oxide residue. In addition, the thermally induced water release of boehmite starts at approx. 100 °C higher than the polymer decomposition and therefore besides the naturally worse efficiency the flame-retardancy will be additionally less effective compared to melamine- or phosphorous-based FRs in a PA12 application.

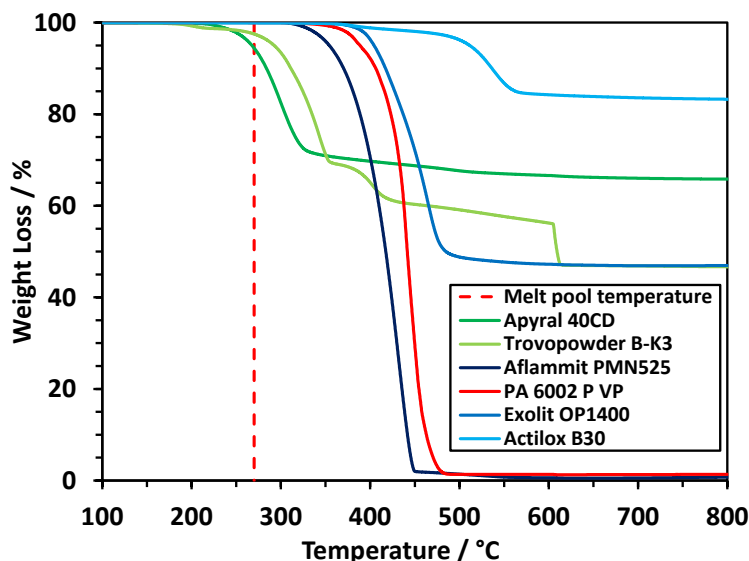


Figure 2: Decomposition behavior of selected FRs in comparison with unfilled PA12 and the LS melt pool temperature determined by TGA under nitrogen (up to 600°C) and oxygen (from 600 °C to 1200 °C) atmosphere

All due to their decomposition behavior suitable FRs for LS were used to produce dry blends as described in the previous section. The composition of each dry blend is shown in Table 4. In general, the total filling ratio is based on the manufacturer’s recommendation for injection molding to achieve a UL94-V0 classification. If no recommendation was given a total filling ratio of 15 wt% was chosen. Because of the typical application of zinc borate (Aflammit PCI 511) and boehmite (Actilox B30) both additives serve mainly as synergists in this work. As discussed before boehmite was not used solely as a FR due to the expected less effectiveness.

Table 4: Composition, filling ratio and notation of each dry blend

Flame-retardant 1	Filling ratio / wt%	Flame-retardant 2	Filling ratio / wt%	Notation
Aflammit PMN 525	15			PMN 525
Versamag	25			Versa
Versamag	10	Aflammit PCI 511	5	Versa / PCI 511
Aflammit PCI 511	15			PCI 511
Nordmin MC-25J	14			MC-25J
Nordmin MC-25J	10	Aflammit PCI 511	5	MC-25J / PCI 511
Nordmin MC-25J	11	Actilox B30	4	MC-25J / B30
GHL PX 90/-2	25			PX 90/-2
Exolit OP1400	15			OP1400
Exolit OP1400	10	Aflammit PCI 511	5	OP1400 / PCI 511
Exolit OP1400	10	Actilox B30	5	OP1400 / B30
Trovopowder B-K3	15			B-K3

In the second step the dry blended FR powders were characterized beginning with the particle size distribution. Figure 3 shows the d10, d50 and d90 percentiles of the measured particle size distributions. In context of LS the particle size has a big impact on the powder flowability, optical properties, surface quality as well as the detail resolution of the produced parts. A high

percentage of fine powder can reduce the powder flowability due to the tendency to form agglomerates and a high percentage of coarse powder can affect the part quality negatively. [10]

It is noticeable that the particle size ( $d_{90} = 226 \mu\text{m}$ ) of the dry blend containing expandable graphite (PX 90/-2) exceeds the maximum layer height of the LS machine and is therefore not a suitable powder for LS. Because most of the examined FRs were developed as additives for compounding and not for dry blending particles sizes are smaller than  $10 \mu\text{m}$ . This leads in comparison with the unfilled PA12 powder ( $d_{10} = 38 \mu\text{m}$ ) to a higher percentage of fine powder indicated by the smaller particle size at  $d_{10}$  percentile (e.g., PMN 525  $d_{10} = 8 \mu\text{m}$ ). Therefore, the powder flowability might be an issue during the processing step. The median as well as the particle size for 90 % of the sample volume are approximately the same, as these depend significantly on the polymer particles.

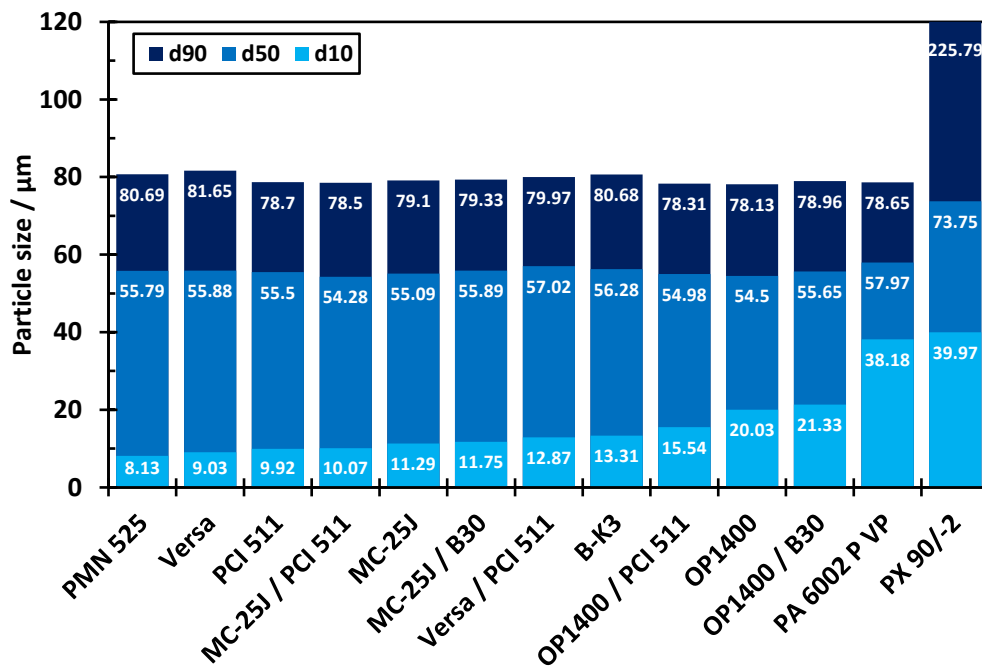


Figure 3: Particle sizes of investigated FR dry blends shown as percentiles ( $d_{10}$ ,  $d_{50}$ ,  $d_{90}$ )

In addition to the particle size distribution, rheological properties of the dry blends were investigated by measuring the melt volume rate (MVR). In general, the coalescence of the polymer particles depends on the viscosity of the melt, which can significantly affect the subsequent properties of the components, such as surface roughness. Factors affecting the viscosity of the entire particle collective include both the average molecular weight of the polymer and the presence of non-meltable particles in the melt. [10]

The results of the measurement are given in Figure 4. In general, the melt volume rate of the dry blends is about  $140 \text{ cm}^3/10\text{min}$ , which is lower by  $50 \text{ cm}^3/10\text{min}$  compared to the unfilled PA12 powder ( $191 \text{ cm}^3/10\text{min}$ ). Since the FRs do not melt at the measurement temperature of  $220 \text{ }^\circ\text{C}$ , they remain as solid particles during the measurement and thus increase the overall viscosity of the melt due to the increase in polymer shear rate. This is also noticeable for the dry blend with the highest filling ratio containing 25 wt% of magnesium hydroxide (Versa), which results in the lowest melt volume rate of approx.  $56 \text{ cm}^3/10\text{min}$ . The powder composition with B-

K3, on the other hand, has a significantly higher melt volume rate of about 300 cm<sup>3</sup>/10min. In addition, brown dots were visible in the plastic strand extruded during the measurement, indicating thermal decomposition of the additive. For this reason, the borosilicate glass foam will be declared as not suitable for LS, as thermal decomposition is to be expected during laser exposure, which has already been made visible by the results of the TGA.

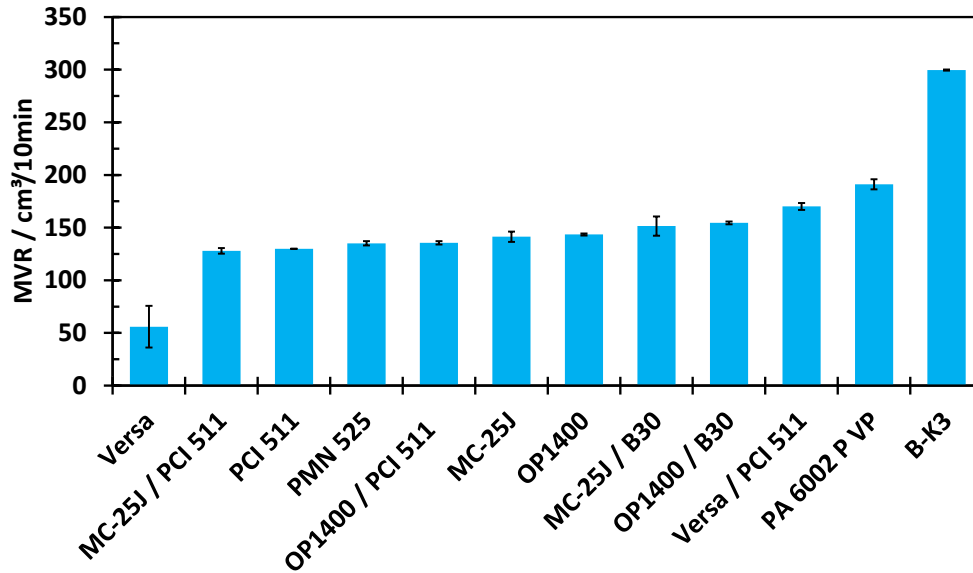


Figure 4: Melt volume rate of investigated FR dry blends of 3 specimens each at 220 °C with 10 kg

Differential scanning calorimetry analyses were performed to study the thermal behavior of each dry blend to determine the melting and crystallization ranges as a function of temperature. For each sample, two heating and cooling cycles were performed in direct succession for an examination independently of the thermal history. In addition, the DSC analysis provides a starting point for adjusting the build temperature in the LS process. [10]

Looking at the results in Figure 5, it is noticeable that the crystallization peak of the FR dry blends is already reached at higher temperatures compared to the unfilled PA 6002 P. The solid particles in the melt serve as nucleating agents and thus cause a shift in the crystallization range [32, 34]. Since only the polymer particles melt and the matrix polymer is the same for all dry blends, the melting point remains unchanged at 187 °C. In addition, the sintering window of the dry blends containing melamine cyanurate is about 6 °C smaller than for OP1400, for example. Possibly, due to the smaller particle size of MC-25J compared to OP1400, there are significantly more solid particles in the melt, which can act as nucleating agents and initiate the crystallization of the polymer.

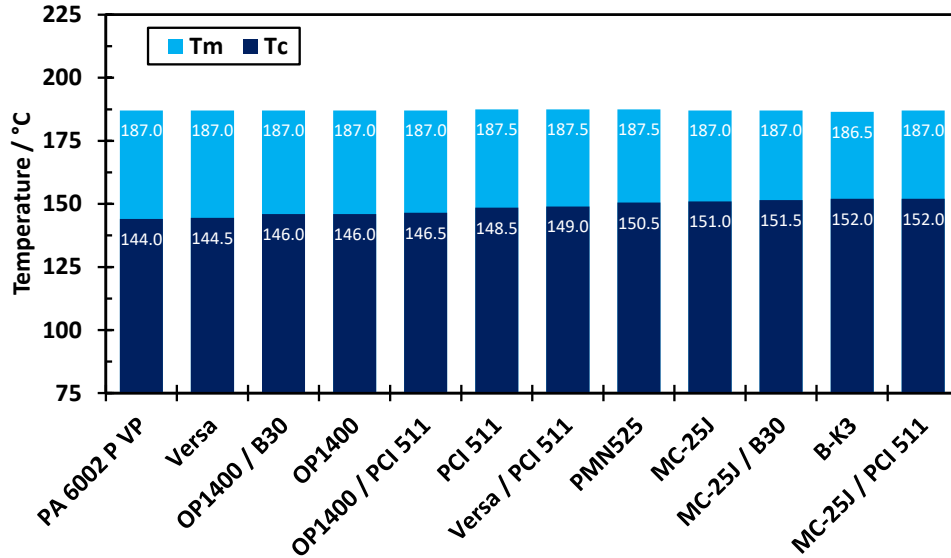


Figure 5: Melt and crystallization temperature of investigated FR dry blends

The DSC diagram (cf. Figure 6) of the dry blend containing OP1400 also shows that the melting enthalpy of the dry blend is lower, since the filler does not melt. This applies for all analyzed blends. Between the first and second cycle, a clear shift between the melting ranges can also be seen, since the as-received polymer powder has a higher crystallinity than the crystal structure resulting from the DSC with a cooling rate of 10 K/min. The melting point of the FR dry blend and the PA12 powder remains the same, as expected. While for the dry blend the recrystallization peak remains unchanged between the first and second cycle, a shift to lower temperature for the virgin PA 6002 P powder is noticeable. It is assumed that the increasing entanglement and elongation of the polymer chains due to post-condensation during the measurement makes crystallite formation more difficult, which accordingly leads to a decrease in crystallinity. [34]

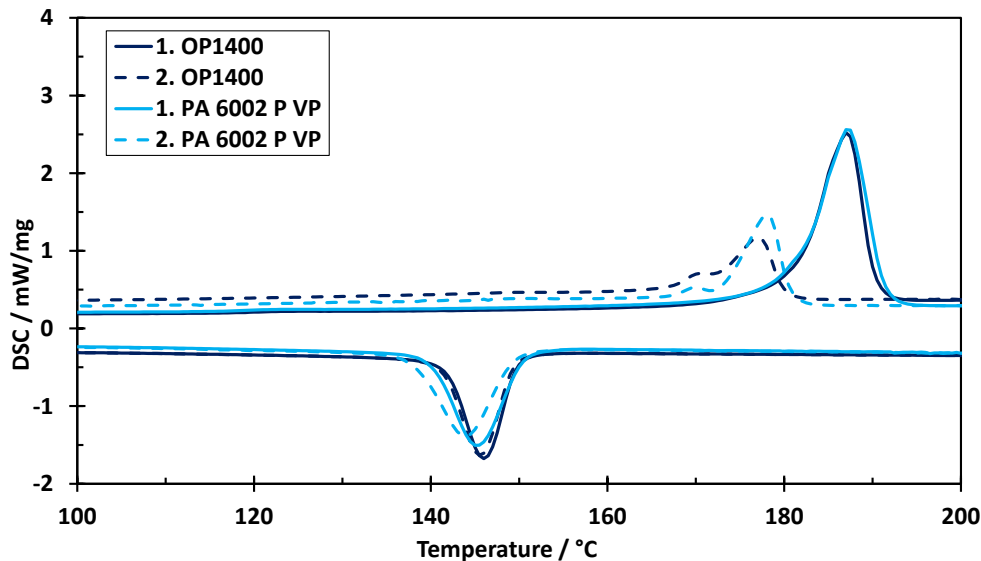


Figure 6: DSC of OP1400 dry blend and neat PA 6002 P powder after first (solid) and second (dashed) temperature cycle; 10 K/min heating/cooling rate

The processability was then investigated within the third step by producing flame-retardancy test specimens on a AMCM customized EOS P395 system. To lower the required quantities of powder for one build process the total build volume of the machine was reduced to 100 x 100 x 100 mm while at the same time build chamber temperatures up to 300 °C can be achieved for processing high-performance polymers. The powder is applied with a roll coater.

First, the powder application of each dry blend was visually inspected and evaluated in terms of application behavior. As expected, the quality of the powder bed decreased with increasing fines content, as this strongly affects the flowability of the powder. Especially with the PMN525 dry blend, which has the highest fines content due to the smallest particle size ( $d_{98} = 8 \mu\text{m}$ ), the application of a homogeneous powder layer without coating defects was not possible (cf. Figure 7 (left)). Although it was still possible to apply a powder layer of sufficient quality for component production due to the installed roll coater, the use of this powder on conventional EOS P3 systems with blade coaters is questionable. This applied for all dry blends with a  $d_{10} < 12 \mu\text{m}$ . The best coating results were achieved using the dry blends containing OP1400, as these have a much lower fines content because of the significantly larger particles ( $d_{90} = 53 \mu\text{m}$ ), as can be seen in Figure 7 (right).



Figure 7: Coated powder of FR dry blends with PMN525 (left) and OP1400 (right)

Afterwards, the build chamber temperature was determined individually for each dry blend to prevent curling prior to the production of flame-retardancy test bars according to the UL94 test standard. In dependency of the dry blend chamber temperatures vary between 168 °C (OP1400) and 172 °C (Versa). Due to the smaller build volume, the length of the test specimens was reduced to 80 mm, accordingly the geometrical dimensions are 80 x 12.5 x 3 mm. The laser parameters for part production were set to an area energy density of 0.0288 J/mm<sup>2</sup>. In specimens manufactured from powder with PMN525, significant unevenness can be observed in the edge areas of the individual layers (cf. Figure 8 (left)), which is due to the reduced flowability of the powder. As can be seen in Figure 8 (right), the powder with OP1400, on the other hand, was able to produce test specimens without geometrical deviations and surface defects.



Figure 8: UL94 V test specimens of FR dry blends with PMN525 (left) and OP1400 (right)

In the fourth step, the flame-retardancy of the individual dry blends was examined. The goal is to achieve a UL94 V-0 rating to enable a future production of for example electronic

components by LS. The following Figure 9 shows the total burning duration of five samples of each dry blend and the corresponding flame-retardancy classification.

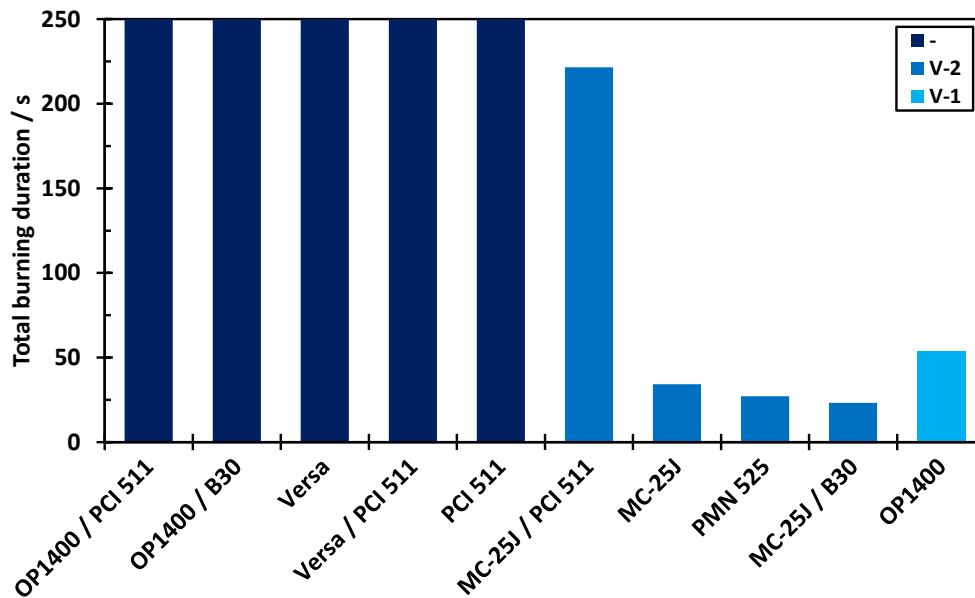


Figure 9: Total burning duration and flame-retardancy classification according to UL94-V test standard of 5 specimens produced by FR dry blends

The results show that at a filler content of maximum 10 wt%, no FR achieved a sufficient protective effect, as the dry blends with OP1400 / PCI 511, OP1400 / B30 and Versa / PCI 511 did not reach any classification due to total burning durations > 250 s. The same applies to the two FRs Versamag (25 wt%) and PCI 511 (15 wt%), which also did not offer sufficient fire protection. MC-25J / PCI 511 is the first dry blend to achieve a flame-retardancy classification, since here the total burning duration of about 221,5 s was below the threshold of 250 s. Due to the strong dripping behavior of the test specimens, which led to the ignition of the cotton wool indicator, this blend was classified in V-2. This can also be seen clearly in Figure 10 (left) from the strand formation in the lower part of the specimens. The test specimens from the melamine cyanurate-containing dry blends MC-25J, PMN 525 and MC-25J / B30 achieved the lowest total burning durations, averaging about 28 s, with the blend containing boehmite as synergist performing best at about 24 s. Although these are well below the 50 s threshold that would be sufficient for a V-0 rating, burning droplets ignited the cotton wool indicator in all tests (see Figure 10 (middle)), resulting in a V-2 rating. The best rating of V-1 was achieved by the test specimens made from powder with OP1400 (15 wt%). The total burning duration of about 53 s was only 3 s above the limit for a V-0 rating. In addition, the formation of a char layer during the tests, which is typical for phosphorus-containing FRs (see Figure 10 (right)), completely prevented the dripping of material from the heat-affected zone and thus the ignition of the indicator.

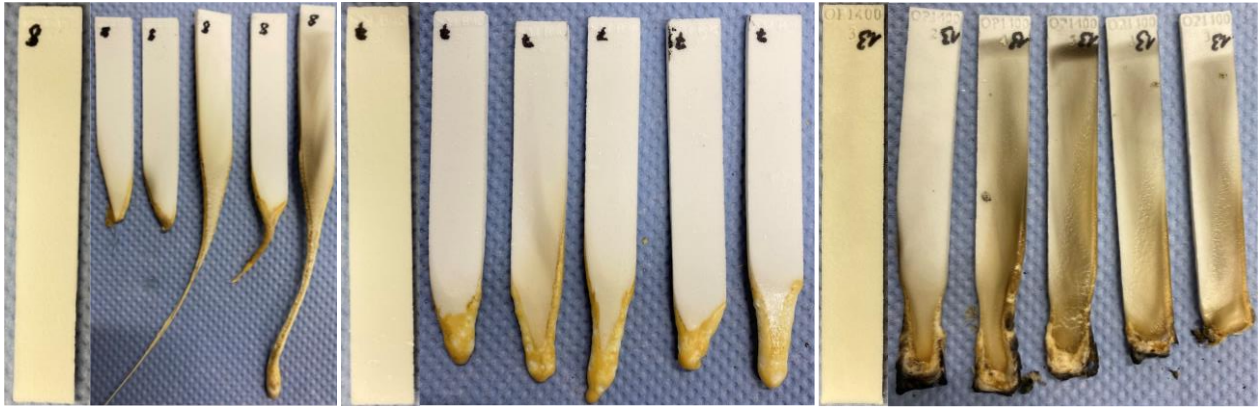


Figure 10: Laser sintered UL94 vertical test specimens with MC-25J/PCI 511 (left), MC-25J/B30 (middle) and OP1400 (right)

In the last and fifth step, aged powder was collected and re-characterized after the respective LS process to evaluate the process stability of the four dry blends that performed best in the flame-retardancy tests. For this purpose, first the melt viscosity was investigated by determining the melt volume rate and then the thermal behavior by means of DSC analysis.

Typically, the reactive chain ends in PA12 powders tend to post-condense during LS due to the long storage at elevated temperatures near the melting point. In this work, the build process took about 4 h due to the reduced build volume. In industrial use, a process usually takes significantly longer. This long process duration leads to longer polymer chains with a correspondingly higher average molar mass. This leads to an increase in melt viscosity, which is reflected in a significant decrease in the melt volume rate. When processing this post-condensed material, there may be an increased occurrence of surface defects, also known as the orange peel effect, which should be avoided. [10, 35]

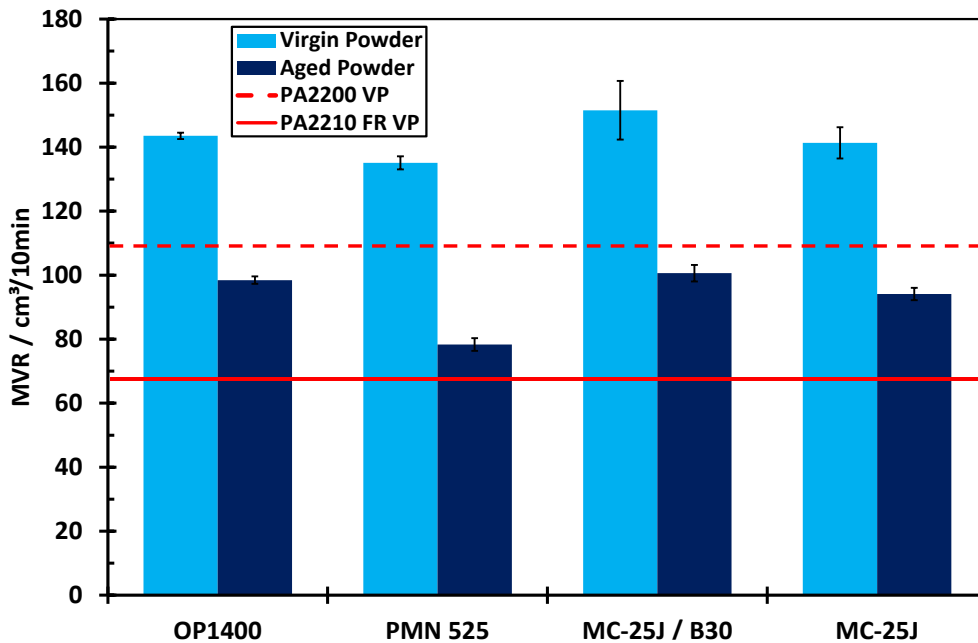


Figure 11: Melt volume rate of virgin and aged FR dry blends with best flame-retardancy compared to unfilled and FR PA12 virgin powder of 3 specimens each at 220 °C with 10 kg

The measurement results of the dry blends shown in Figure 11 are compared with unfilled standard PA12 powder (PA 2200 VP) and the commercially available PA12 FR virgin powder (PA 2210 FR VP). In virgin state the dry blends have a higher melt volume rate than PA 2200 VP due to the use of the recycling optimized PA 6002 P as polymer matrix. The effect of polycondensation and the resulting increase in viscosity is visible for all dry blends, as the melt volume rate of the aged powder is reduced by about 35 % on average and therefore lower than the rate of PA 2200 VP. However, the rates of the aged powder are still significantly higher than those of the PA 2210 FR VP. Since no surface defects occurred during the processing of the PA 2210 FR VP in previous investigations, it can be assumed that these will also not occur when using the aged powder of the dry blends.

In Figure 12 and Figure 13 the DSC diagrams of both dry blends with the best results in the flame-retardancy tests (OP1400, MC-25J / B30) in virgin and process-aged state are shown. Two measurement runs were performed for each sample. As expected, the melting point of both materials shifted to lower temperatures (approx. 177 °C) due to the change in crystallinity of the polymer caused by the deviating cooling rate after the first cycle. In comparison between virgin and aged powder the crystallization did not change significantly, so that it can be assumed that the solid particles of the FR were not affected by the LS process. In future investigations with aged material, this assumption must be confirmed by further flame-retardancy tests.

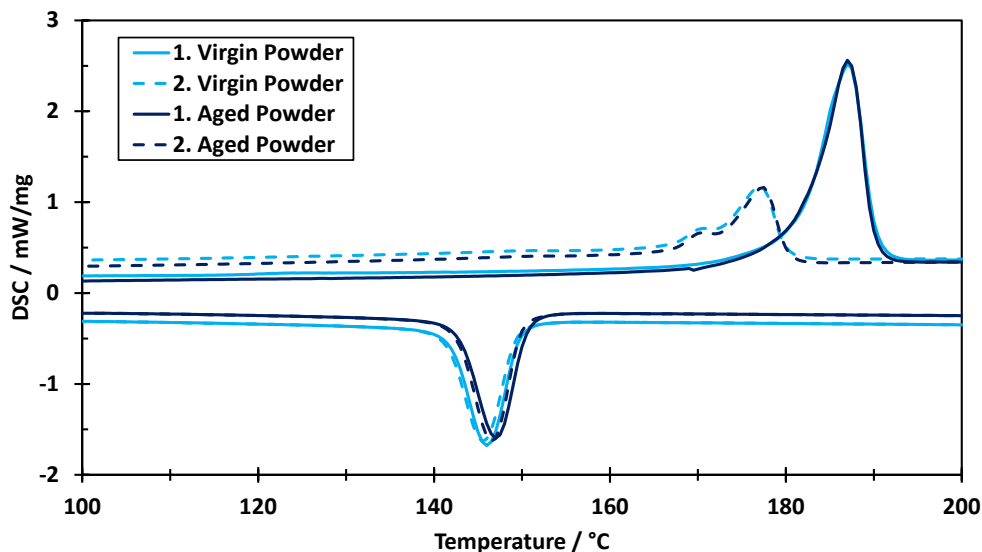


Figure 12: DSC-Analysis of PA12 powder with OP1400 in virgin as well as process aged state after first (solid) and second (dashed) temperature cycle; 10 K/min heating/cooling rate

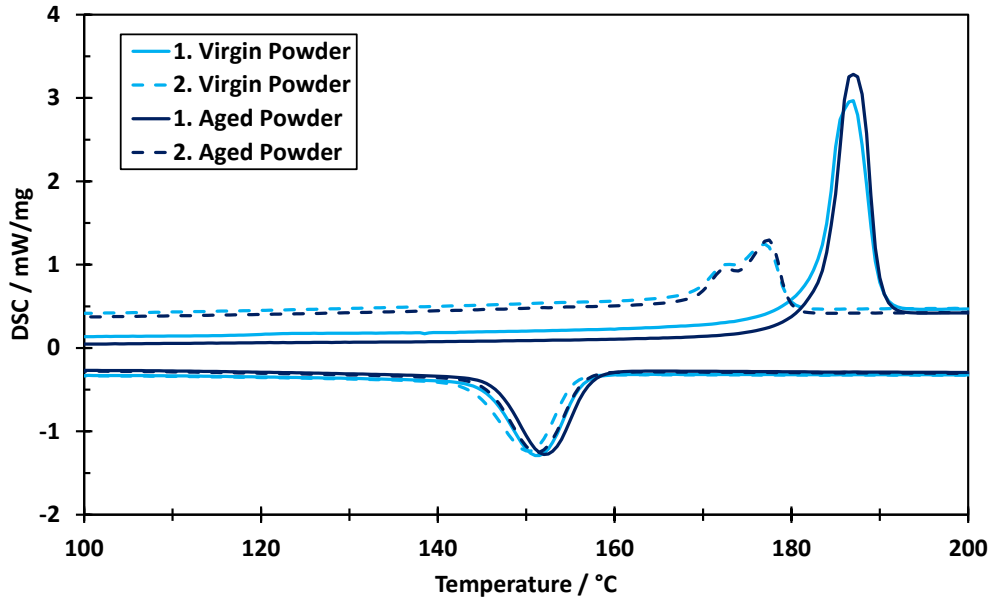


Figure 13: DSC-Analysis of PA12 powder with MC-25J / B30 in virgin as well as process aged state after first (solid) and second (dashed) temperature cycle; 10 K/min heating/cooling rate

### Summary

In this work, various FRs, e.g., aluminum hydroxide, boehmite, phosphorous and melamine cyanurate, were investigated for their suitability in LS. These additives were dry blended with the commercially available INFINAM PA 6002 P PA12 (optimized for reduced aging effects) powder with total filling ratios ranging from 11 wt% up to 25 wt%. The dry blends were then subjected to a five-step evaluation process, ranging from decomposition behavior and powder characterization to processability during LS, achieved fire protection and process stability. After each step, the FRs and later the dry blends were evaluated to determine if the step specific requirements were met.

As the mode of action of all FRs is initiated by thermal decomposition the decomposition behavior was analyzed first by thermogravimetric analysis. It was shown that aluminum hydroxide is not suitable for LS since a mass loss of > 5 % was measured at the assumed melt pool temperature of 270 °C, therefore the additive would already decompose to a certain amount in the process due to the energy impact of the laser. Measuring the particle size distribution of the dry blends further revealed, that expandable graphite is also not suitable for LS, due to particle sizes larger than the maximum layer height of 180 µm of the EOS P3 system. During the powder characterization, including the measurement of the melt volume rate and a DSC analysis, it was found that the thermal stability of borosilicate glass foam is also not sufficient to be used in LS. When processing the remaining dry blends, it became clear that especially the powder flowability of zinc borate, melamine cyanurate and magnesium hydroxide due to high fines content caused by the small particle size of the FRs can limit the application behavior in systems with blade coaters. Since the AMCM customized EOS P3 system used in this work has a roll coater, it was still possible to produce flame-retardancy test specimens. However, the reduced powder flowability has in some cases led to significant geometrical deviations of the test specimens. The subsequent fire protection tests carried out in accordance with UL94 V test standards showed that dry blends with a total filling ratio of 15 wt%, with the FR additive with the highest filler content being only 10 wt%, were not sufficient for any classification. Dry blends with melamine cyanurate showed excellent fire

protection properties, but the occurrence of burning droplets resulted only in a V-2 classification. The best properties were obtained with the phosphorus-containing FR Exolit OP1400, which achieved a V-1 classification at a wall thickness of 3 mm and a filler content of 15 wt%. In addition, subsequent measurements of melt viscosity and thermal behavior suggest that both the aged powder of the dry blends with melamine cyanurate and with OP1400 may be suitable for further process iterations.

In future studies, the process stability of the two most promising FRs, melamine cyanurate and OP1400, must be confirmed by further fire protection tests with a mixture of process-aged and virgin powders. Furthermore, the aim is to achieve a V-0 rating by improving the dripping behavior when using melamine cyanurate and by increasing the filler content of OP1400. Testing of mechanical properties and the use of additional synergists is also part of future investigations.

### References

- [1] AMFG Autonomous Manufacturing. “Die Evolution des selektiven Lasersintern (SLS): Neue Technologien, Materialien und Anwendungen,” [Online]. Available: <https://amfg.ai/de/2020/02/02/die-evolution-des-selektiven-lasersintern-sls-neue-technologien-materialien-und-anwendungen/> (accessed Jan. 25, 2023).
- [2] E. D. Weil and S. V. Levchik, *Flame Retardants for Plastics and Textiles*. München: Hanser Verlag, 2016.
- [3] Henri Vahabi, Mohammad Reza Saeb, and Giulio Malucelli, *Analysis of Flame Retardancy in Polymer Science*. Elsevier, 2022, doi: 10.1016/C2020-0-01599-9.
- [4] S. S. Ray and M. Kuruma, *Halogen-Free Flame-Retardant Polymers*. Springer Nature Switzerland AG, 2020.
- [5] Y. F. Lv, W. Thomas, R. Chalk, and S. Singamneni, “Flame retardant polymeric materials for additive manufacturing,” *Materials Today: Proceedings*, vol. 33, pp. 5720–5724, 2020, doi: 10.1016/j.matpr.2020.05.081.
- [6] K. Schneider, K. Wudy, and D. Drummer, “Flame-Retardant Polyamide Powder for Laser Sintering: Powder Characterization, Processing Behavior and Component Properties,” *Polymers*, early access. doi: 10.3390/polym12081697.
- [7] EOS GmbH - Electro Optical Systems. “PA 2210 FR for EOSINT P,” [Online]. Available: <https://additivemanufacturingllc.com/wp-content/uploads/2015/04/PA-2210-FR.pdf> (accessed Sep. 08, 2023).
- [8] 3D Systems. “DuraForm FR1200 TDS,” [Online]. Available: [https://support.3dsystems.com/s/article/materials-duraform-fr1200?language=en\\_US](https://support.3dsystems.com/s/article/materials-duraform-fr1200?language=en_US) (accessed May. 17, 2023).
- [9] S. Yu, A. Tan, W. M. Tan, X. Deng, C. L. Tan, and J. Wei, “Additive manufacturing of flame retardant polyamide 12 with high mechanical properties from regenerated powder,” *RPJ*, 2023. [Online]. Available: <https://www.emerald.com/insight/content/doi/10.1108/RPJ-05-2022-0146/full/pdf?title=additive-manufacturing-of-flame-retardant-polyamide-12-with-high-mechanical-properties-from-regenerated-powder> (accessed Jun. 27, 2023)
- [10] M. Schmid, *Lasersintern (LS) mit Kunststoffen: Technologie, Prozesse und Werkstoffe*. München: Hanser, 2022.
- [11] J. Troitzsch and E. Antonatus, *Plastics flammability handbook: Principles, regulations, testing, and approval*, 4th ed. Cincinnati: Hanser Publications, 2021.

- [12] Umweltbundesamt. “*Bromierte Flammschutzmittel - Schutzengel mit schlechten Eigenschaften*,” [Online]. Available: <https://www.umweltbundesamt.de/sites/default/files/medien/publikation/long/3521.pdf> (accessed Aug. 5, 2021).
- [13] Andreas Wegner, “*Theorie über die Fortführung von Aufschmelzvorgängen als Grundvoraussetzung für eine robuste Prozessführung beim Laser-Sintern von Thermoplasten*,” Dissertation, Maschinenbau und Verfahrenstechnik, Universität Duisburg-Essen, Duisburg, 2015. [Online]. Available: [https://duepublico2.uni-due.de/servlets/MCRFileNodeServlet/duepublico\\_derivate\\_00038726/Wegner\\_Andreas\\_Diss.pdf](https://duepublico2.uni-due.de/servlets/MCRFileNodeServlet/duepublico_derivate_00038726/Wegner_Andreas_Diss.pdf)
- [14] H. Vahabi, F. Laoutid, M. Mehrpouya, M. R. Saeb, and P. Dubois, “Flame retardant polymer materials: An update and the future for 3D printing developments,” *Materials Science and Engineering: R: Reports*, vol. 144, p. 100604, 2021, doi: 10.1016/j.mser.2020.100604.
- [15] Nabaltec AG, “*Mineral based flame retardancy with metal hydrates*,” Dec. 2022. [Online]. Available: [https://nabaltec.de/fileadmin/user\\_upload/07\\_presse/Mediathek/Web\\_Brochure\\_Mineral\\_based\\_Dec-2022.pdf](https://nabaltec.de/fileadmin/user_upload/07_presse/Mediathek/Web_Brochure_Mineral_based_Dec-2022.pdf) (accessed Feb. 2, 2023)
- [16] Nabaltec AG, “*Apyral Aluminiumhydroxid*,” (n.d.). [Online]. Available: <https://nabaltec.de/produkte/aluminiumhydroxid/> (accessed Feb. 2, 2023)
- [17] R.J. Marshall Company. “*Fire Retardants and Smoke Suppressants*,” [Online]. Available: [https://mat.rjmarshall.com/wp-content/uploads/sites/2/2021/04/MAT\\_Brochure\\_Apr\\_2021-web.pdf](https://mat.rjmarshall.com/wp-content/uploads/sites/2/2021/04/MAT_Brochure_Apr_2021-web.pdf) (accessed Feb. 3, 2023).
- [18] Clariant. “*PDS Exolit OP 1400*,” [Online]. Available: <https://www.clariant.com/de/Solutions/Products/2014/06/27/09/05/Exolit-OP-1400?p=1> (accessed Jun. 27, 2023).
- [19] Clariant. “*Exolit OP 1400 Flame Retardant*,” [Online]. Available: <https://www.clariant.com/de/Solutions/Products/2014/06/27/09/05/Exolit-OP-1400> (accessed Feb. 3, 2023).
- [20] THOR GmbH, “*AFLAMMIT PMN 525*,” Sep. 2019. Accessed: Feb. 3, 2023.
- [21] Nordmann, Rassmann GmbH, “*Nord-Min MC-25J*,” Apr. 2019. Accessed: Feb. 3, 2023.
- [22] THOR GmbH, “*PDS Aflammit PCI 511*,” Sep. 2012. Accessed: Feb. 3, 2023.
- [23] Trovotech. “*Flammschutz TROVOpowder B*,” [Online]. Available: <https://www.trovotech.com/index.php/de/flammschutz-abrieb> (accessed Feb. 3, 2023).
- [24] Trovotech, “*TROVOpowder B-K3-04 12 03*,” Jan. 2021. Accessed: Feb. 3, 2023.
- [25] F. Tomiak, K. Rathberger, A. Schöffel, and D. Drummer, “Expandable Graphite for Flame Retardant PA6 Applications,” *Polymers*, early access. doi: 10.3390/polym13162733.
- [26] Luh GmbH, “*PDS GHX PX 90/-1 HT 230*,” Feb. 2022. Accessed: Feb. 3, 2023.
- [27] *Kunststoffe - Thermogravimetrie (TG) von Polymeren*, 11358-1, Deutsches Institut für Normung e. V., Berlin, Oct. 2014.
- [28] *Partikelgrößenanalyse - Bildanalyseverfahren: Teil 2: Dynamische Bildanalyseverfahren*, 13322-2, International Organization for Standardization, Berlin, Dec. 2021.
- [29] Sympatec GmbH. “*Dynamische Bildanalyse*,” [Online]. Available: <https://www.sympatec.com/de/partikelmesstechnik/sensoren/dynamische-bildanalyse/> (accessed Feb. 13, 2023).
- [30] *Kunststoffe – Bestimmung der Schmelze-Massefließrate (MFR) und der Schmelze-Volumenfließrate (MVR) von Thermoplasten – Teil 1*, 1133-1, Deutsches Institut für Normung e. V., Berlin, Oct. 2022.
- [31] *Kunststoffe - Dynamische Differenz-Thermoanalyse*, 11357-1, Deutsches Institut für Normung e. V., Berlin, Feb. 2017.
- [32] G. W. Ehrenstein, *Thermische Analyse: Brandprüfung, Wärme- und Temperaturleitfähigkeit, DSC, DMA, TMA* (Erlanger Kunststoff-Schadensanalyse). München: Hanser, 2020.

- [33] L. Jianjun and O. Yuxiang, *Theory of Flame Retardation of Polymeric Materials*. Berlin, Boston: De Gruyter, 2019. [Online]. Available: [http://www.degruyter.com/search?f\\_0=isbnissn&q\\_0=9783110349269&searchTitles=true](http://www.degruyter.com/search?f_0=isbnissn&q_0=9783110349269&searchTitles=true) (accessed: Jun 27, 2023)
- [34] G. W. Ehrenstein, *Polymer-Werkstoffe: Struktur - Eigenschaften - Anwendung*, 3rd ed. München: Hanser, 2011.
- [35] T. A. Osswald, E. Baur, and N. S. Rudolph, *Plastics handbook: The resource for plastics engineers*, 5th ed. Cincinnati Ohio: Hanser Publications, 2019.